Journal of Crystal Growth 310 (2008) 3154–3158

Contents lists available at ScienceDirect

Journal of Crystal Growth

journal homepage: www.elsevier.com/locate/jcrysgro

Mechanism for spontaneous growth of GaN nanowires with molecular beam epitaxy ☆

K.A. Bertness *, A. Roshko, L.M. Mansfield, T.E. Harvey, N.A. Sanford

National Institute of Standards and Technology Optoelectronics Division, Mail Stop 815.04325 Broadway, Boulder, CO 80302, USA

ARTICLE INFO

Article history:
Received 15 October 2007
Received in revised form
20 February 2008
Accepted 24 March 2008
Communicated by E. Calleja
Available online 1 April 2008

PACS:
81.07.Bc
81.15.Hi
81.05.Ea
68.37.Hk
68.35.Ct

Keywords:
A1. Nanostructures
A3. Molecular beam epitaxy
B1. Nitrides
B2. Semiconducting III–V materials

ABSTRACT

Although most semiconductor nanowires are grown via the vapor–liquid–solid mechanism, we present evidence that GaN nanowires form because of thermodynamically driven variations in surface sticking coefficients on different crystallographic planes under certain conditions in molecular beam epitaxy (MBE). Specifically, the wires nucleate spontaneously and then propagate because the sticking coefficient on the (0 0 0 1) *c*-plane is higher than that on the {1 1 0 0} *m*-plane under conditions of high temperature (810–830 °C) and high N_2 overpressure. Elemental Ga droplets are unstable under these growth conditions and therefore cannot act as catalytic sites for nanowire growth. This conclusion is based on differences in morphology and growth conditions for GaN nanowires grown with and without catalysts, whether the catalysts are extrinsic metals or Ga droplets. The spontaneous MBE growth of GaN nanowires is therefore shown to be distinct in mechanism from that of the growth of most semiconductor nanowires.

Published by Elsevier B.V.

1. Introduction

The growth of semiconductor nanowires is a rapidly expanding field driven in part by the unique functionality of nanowires and their high crystalline quality despite high degrees of epitaxial or thermal mismatch strain, particularly for group III nitride growth. The majority of these nanowires are grown with catalyst nanoparticles, usually a metal such as Au or Ni, which enhances growth at the nanowire tip through supersaturation of reactant species within the catalyst droplet. Early observations of GaN nanowires grown with molecular beam epitaxy (MBE) were explained with a self-catalysis mechanism [1], with Ga droplets playing the role of the catalyst metal. In addition, there are a number of direct-reaction nanowire growth methods that also appear to be consistent with the propagation of the nanowires through the formation of a Ga droplet. While catalyst droplets have been directly observed on nanowire tips after catalytic and direct-reaction growth of GaN nanowires [2,3], they have never been observed following spontaneous growth by MBE.

As we will show, the differences in morphology and growth conditions for these growth processes are sufficiently large that they indicate a distinct mechanism for spontaneous nanowire growth. We have previously proposed [4–6] an alternative model in which the nanowires propagate because of a higher sticking coefficient for the group III atoms (e.g., Ga) on the nanowire tip relative to the sticking coefficient on the *m*-plane sidewalls. This mechanism is illustrated schematically in Fig. 1. When the sticking coefficient is much larger on the tip than on the sidewalls, Ga atoms that impinge on the growing nanowire at the very tip or within a surface diffusion length of the tip will incorporate there. Atoms that land farther down the sidewall will mostly desorb into the chamber and not contribute to nanowire growth. The relative magnitude of the sticking coefficients and surface diffusion lengths naturally depends on growth conditions such as temperature and N species flux. We will show that the growth behavior is consistent with the expected trends for these parameters. The initial nucleation mechanisms vary, but one mode most commonly observed in our work is the formation of a seed crystal in the center of a spontaneously formed pit [5]. The data also show that regardless of the seed crystal nucleation mechanism, under typical nanowire MBE growth conditions, the growth of a nanowire from a seed crystal proceeds through the differential sticking coefficient mechanism.

☆ Contribution of an agency of the U.S. government; not subject to copyright.

* Corresponding author. Tel.: +1 303 497 5069; fax: +1 303 497 3387.
E-mail address: bertness@boulder.nist.gov (K.A. Bertness).

0022-0248/$ - see front matter Published by Elsevier B.V.
doi:10.1016/j.jcrysgro.2008.03.033

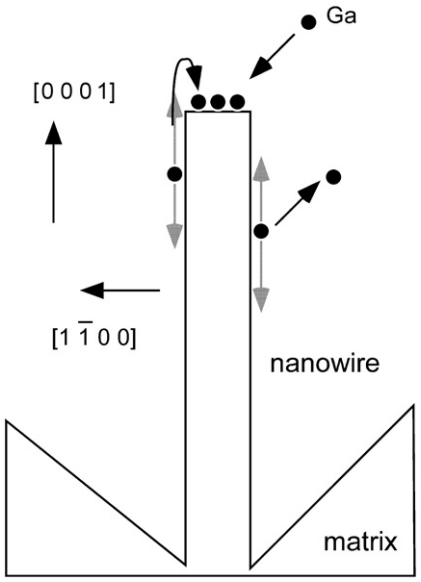

Fig. 1. Schematic of differential sticking coefficient mechanisms for spontaneous nanowire growth in MBE. Ga atoms that impinge on the nanowire tip or within a surface diffusion length of the tip (illustrated on the left side of the wire) will incorporate at the tip; adatoms arriving farther down the sides (illustrated on the right side of the wire) are likely to desorb rather than incorporate. The nanowire is shown growing out of a GaN matrix layer, as we typically observe for MBE growth on AlN buffers on Si (1 1 1) substrates. The sidewalls of the matrix pits are {1 $\bar{1}$ 0 2} planes.

2. Experimental procedure

The nanowires were grown by MBE under conditions of high substrate temperature (810–830 °C) and high N_2 plasma flux. These temperatures are sufficiently high that Ga re-evaporation occurs during growth. The growth chamber pressure was approximately 2.6×10^{-3} Pa (2.0×10^{-5} Torr), almost all of which was N species from the radio frequency (RF) plasma N_2 source. The growth rates for the nanowires were from 0.1 to 0.2 μm/h. The typical beam equivalent pressure (BEP) for Ga was 1.3×10^{-5} Pa (1.0×10^{-7} Torr) , although our experience indicated that the sensitivity of the pressure gauge to Ga varied by a factor of two depending on the age of the active element. The nanowires illustrated in this paper were primarily grown on Si substrates with (1 1 1) orientation, and some examples of growth on Si (1 0 0) are also presented. We grew a thin AlN buffer layer between the Si substrate and GaN nanowire layer; the buffer layer thickness varied from 30 to 120 nm. Additional details of the growth conditions for the GaN nanowires have been reported elsewhere [4]. The morphology of the nanowires has been examined with field-emission scanning electron microscopy (FESEM). X-ray diffraction on as-grown nanowire assemblies was carried out in a triple-axis diffractometer operated in double-axis mode (that is, with an "open" or rocking curve detector). Azimuthal (phi) scans about the specimen normal were obtained while the 2θ (the detector angle relative to X-ray beam) and ω (angle of the sample plane relative to X-ray beam) were held at the GaN (1 0 5) diffraction condition. The scans were acquired piece-wise to allow reoptimization of ω (but not 2θ) at each azimuthal peak; this corrects for the specimen tilt relative to the stage.

The growth temperature range over which we observe nanowire growth is approximately from 800 °C to 840 °C. Below this temperature the film no longer contains isolated nanowires, and by 760 °C it resembles a pitted, continuous film. There is variation from group to group on the center of the range of substrate temperatures for GaN nanowire growth with MBE [7–11], such that the total range of reported temperatures extends from 720 to 900 °C, but no one group has reported successful growth over a temperature range broader than 40 °C. The variation from system to system is most likely due to shifts in the growth window with variations in plasma source products, Ga flux, and temperature calibration, none of which are easily measured to high accuracy. As previously reported [4], we calibrate our growth temperatures with a conventional optical pyrometer on a bare silicon wafer (which has constant and known emissivity) against the filtered black body radiation emitted from the back side of the wafer through a light pipe in the manipulator. This back-side pyrometer, which is insensitive to emissivity changes due to growth deposits on the front side of the substrate, is then used throughout the run to monitor substrate temperature. The estimated uncertainty for this method is 8 °C.

3. Results

Because no external catalysts were present in the MBE growths, the first question to address is whether evidence exists for self-catalysis during MBE growth, that is, the formation of nanometer-scale Ga droplets that facilitate the familiar vapor–liquid–solid mechanism. Catalyst particles are frequently observed after catalyst nanowire growth has been terminated and the specimen removed for examination [2,3,12]. As shown for representative specimens in Fig. 2, residual Ga droplets are absent in post-growth analysis of MBE-grown nanowires. The high ratio of active N to Ga required to nucleate and propagate spontaneous nanowire growth argues against the stability of Ga droplets, which would readily be consumed through reaction with excess N.

To counter the argument that the droplets might exist during growth, but become incorporated into the nanowire as it cools in the N-only environment typically following growth, in Figs. 3 and 4 we illustrate the morphology that results from cooling nanowires under Ga flux. For the run illustrated in Fig. 3, the wafers were cooled with the Ga shutter open from growth temperature of 815 °C to below 300 °C with the N_2 plasma source still operating. Instead of preserving or adding to a droplet as the growth temperature decreases and therefore Ga re-evaporation decreases, the Ga continues to incorporate with N as a solid crystalline overcoat on the nanowire sidewalls. In some cases side branches and faceted ends form that retain the six-fold symmetry of the original nanowire. Results of an additional, more stringent cooling test are shown in Fig. 4. For this run, the nanowires were cooled from the growth temperature of 815 °C down to 650 °C under the same Ga flux used during growth but with the N_2 plasma source shuttered, RF power turned off, and N_2 gas flow diverted from the chamber at the same time that cooling was begun. The time of exposure to Ga flux alone was approximately 90 s, by which point the background pressure in the chamber was below 4×10^{-6} Pa. As can be seen in FESEM images, there is no indication of Ga accumulation on most of the nanowires, and none contain catalyst-sized droplets. Some of the larger wires (Fig. 4(b)) show a slight bulge on the tips that is only a fraction of the total wire diameter. This amount is consistent with decomposition of the crystal due to being maintained in vacuum at high temperature after the N_2 supply is removed and accumulation of Ga intercepted by the larger wires during the final cooling period.

MBE-grown GaN nanowires are unusual in that they consistently form with hexagonal cross-section (see Fig. 2). We have previously shown that the sidewalls of the nanowires are *m*-planes, with indices in the {1 $\bar{1}$ 0 0} family, and that the growth axis coincides with the GaN *c*-axis direction [5]. This stands in

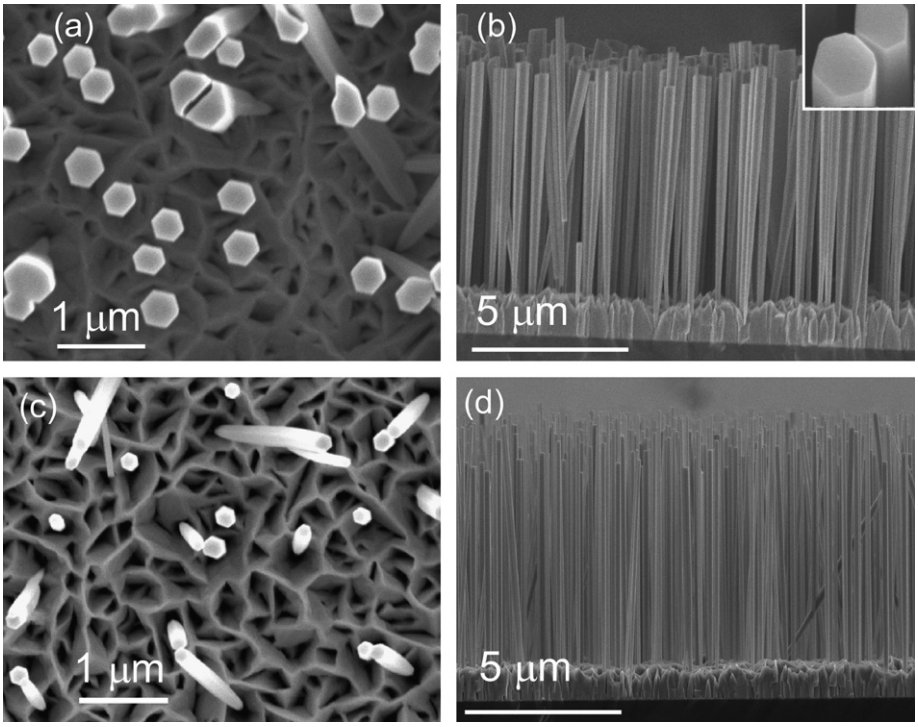

Fig. 2. FESEM top views (a–c) and side views (b–d) of the morphology for two spontaneous nanowire runs showing the hexagonal cross-section and upright growth habit. The upper set of micrographs (a,b) shows the increase in diameter during growth that results when nanowires are close enough to recapture Ga atoms desorbing from neighboring wires. A tilted close-up of the nanowire tips shows that no Ga droplets are present after growth [inset in (b)], nanowire diameter about 500 nm.

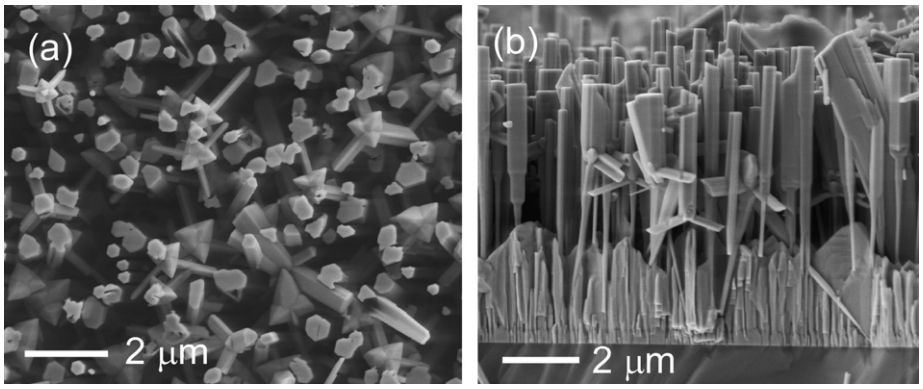

Fig. 3. FESEM top view (a) and side view (b) of GaN nanowire growth in which the nanowires were cooled to less than 300 °C under Ga and N flux, as described in the text. If Ga droplets had been present during growth, they would have been expected to persist and even enlarge because Ga re-evaporation is reduced at lower temperatures. Instead the growth of GaN continues in crystalline layers with side branches (top view) and clear overcoats (side view).

sharp contrast to catalyst-grown nanowires, which form with a variety of cross-sections including circular [3], triangular [13], irregular cross-sections with rough sidewalls, thin ribbons [14], and variable ratios of hexagonal, rectangular and triangular [15]. Catalyst-grown nanowires typically grow along the *a*-axis direction, although *m*-axis and *c*-axis growths also occur. Unless the catalysts are well separated and growth is unusually slow, catalytic and self-catalytic wires grow in all directions from a substrate, seed droplet, seed crystal or chamber wall [2,16,17]. Catalytic-grown material frequently resembles steel wool or filamentary root growth. In contrast to this variety, MBE-grown nanowires are almost exclusively hexagonal, mostly normal to the substrate surface and have faceted sidewalls and a straight, angular appearance even when high density causes them to coalesce. For completeness, we note that spontaneous nanowires may coalesce into larger structures and occasionally grow at a steep angle to the substrate normal. The tilted structures are much larger in volume than the typical nanowire and contain crystallographic defects not found in nanowires. Two of them have been examined with electron backscatter diffraction to reveal that the growth axis is also the *c*-axis direction. Although their formation mechanism may have similarities to that of true nanowires, we will not be addressing their properties or growth mechanisms in this paper.

The consistent crystallographic symmetry of spontaneously nucleated nanowires implies a thermodynamic driving force in their formation. We note that there are also other growth methods that produce prismatic GaN crystals with hexagonal cross-section, including nanowire growth with hot wall epitaxy [18], patterned epitaxial growth of GaN nanowires [19,20], and bulk growth methods [21]. The hexagonal shape of spontaneously formed nanowires is preserved despite the variety of nucleation

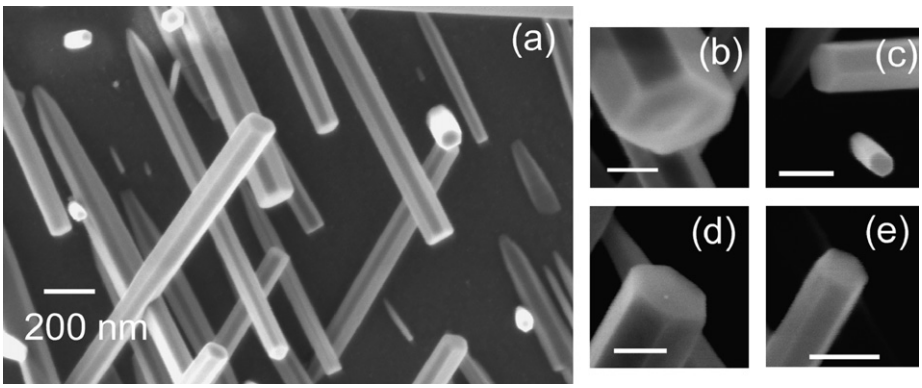

Fig. 4. FESEM views of GaN nanowires cooled under Ga flux without nitrogen overpressure (see text for details). (a) Low-magnification view, (b)–(e) higher magnification images of ends, marker bar of 100 nm. All the nanowires are free of catalyst-size Ga droplets. (b) illustrates a small Ga surplus accumulated during the cooling phase.

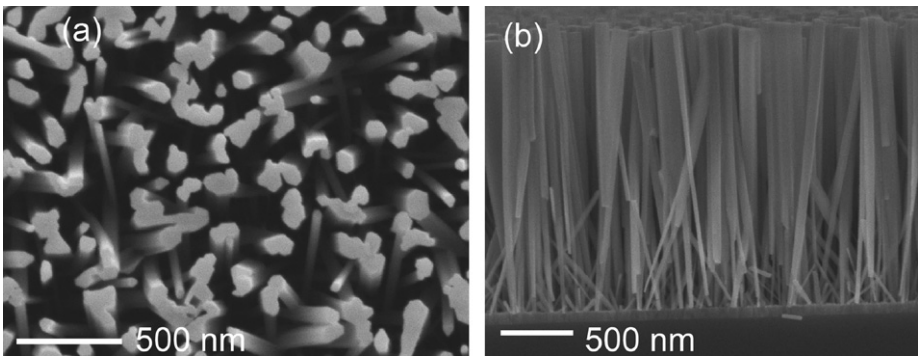

Fig. 5. FESEM top view (a) and side view (b) of MBE nanowire growth on Si (1 0 0). Relative azimuthal orientation is more random and nucleation more dense than for nanowires grown on Si (1 1 1), leading to high coalescence and increasing diameter as growth progresses. The hexagonal cross-section is visible for a few isolated wires in the top view, and coalesced wires retain angular sidewalls. The AlN buffer is visible in the side view as a medium tone layer of uniform thickness about 100 nm thick. Nanowires nucleate at the AlN–GaN interface.

conditions used by different groups growing MBE nanowires. Our proposed model explains these observations because the propagation mechanism of differential sticking coefficients is independent of the nucleation method. To the extent that self-catalysis and catalyst-based growth of nanowires occasionally (but not consistently) produce the same morphology as observed for noncatalytic MBE growth, it is likely to be where the growth conditions strongly suppress growth on *m*-plane sidewalls.

Specific examples of the variety of noncatalytic nucleation conditions include seeded growth [9], growth on Si (1 1 1) [10–22], growth on sapphire or Si (1 1 1) [1–8], growth on Si (1 0 0) [23], growth with intentional surface nitridation [10], growth with AlN buffer layers [5,24,25] and growth without AlN buffer layers [26,27]. In Fig. 5 we illustrate recent results for nanowire growth on Si (1 0 0) substrates. On this surface the nucleation process produces dense, small nanowires that increase in diameter as growth progresses. Coalescence alters the hexagonal cross-section but the angular sidewalls remain, and the few isolated nanowires show clear three-fold and six-fold symmetry. The relative azimuthal orientation for nanowires grown on Si (1 0 0) is more random than that for nanowires grown on Si (1 1 1), in which the GaN $\langle 11\bar{2}0 \rangle$ direction is aligned with the Si $\langle 1\bar{1}0 \rangle$ direction. X-ray diffraction of the nanowire ensembles (Fig. 6) indicates a tendency for nanowires grown on Si (1 0 0) to align along two azimuthal directions with a relative separation of 90°, which corresponds to two equivalent directions in the Si lattice. (Because of the six-fold symmetry of GaN, this relative orientation of the GaN and Si is also equivalent to two GaN orientations with relative azimuthal angle of 30°.) This azimuthal dependence results in phi-scans for asymmetric diffraction peaks that exhibit weak 12-fold

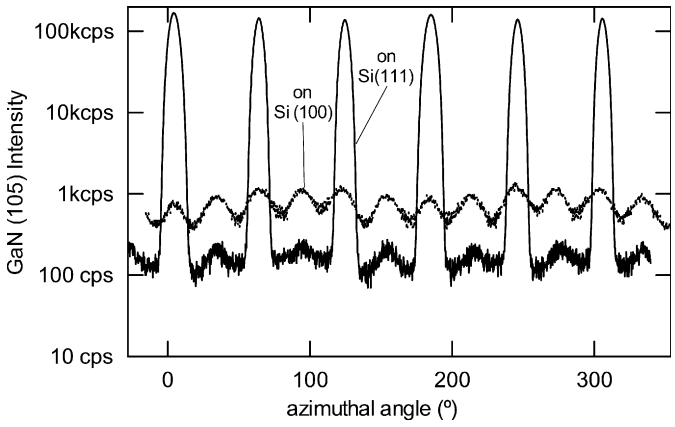

Fig. 6. Azimuthal angle dependence (phi scan) of the intensity of the GaN (1 0 5) X-ray diffraction peak for GaN nanowires grown on Si (1 0 0) and Si (1 1 1) substrates. The nanowire lengths are 2 and 3 μm, respectively. Nanowires grown on Si (1 1 1) show a much higher degree of relative azimuthal alignment and a 1000:1 domination of one orientation relative to the silicon substrate. These results taken in combination with the identical hexagonal morphology of individual nanowires on both substrate types indicate that nucleation and propagation are independent processes under these growth conditions.

symmetry, similar to that reported for MBE film growth on Si (1 0 0) [28]. The relative azimuthal alignment for nanowires grown on Si (1 1 1) is much stronger, producing essentially six-fold phi-scans, as would be expected for single-crystalline, *c*-axis GaN. These results taken in combination with the identical hexagonal morphology of individual nanowires on both substrate types

indicate that nucleation and propagation are independent processes under these growth conditions.

Another consistent difference between catalytic growth and spontaneous growth of nanowires is that the diameter is more consistent and the length is widely variable with the former, while for the latter the diameter varies dramatically and yet the length is consistent to within 10%. Their uniform length is an indication that the spontaneous nanowires nucleate only at the AlN buffer layer, as confirmed by transmission electron microscopy [6] and cross-sectional FESEM. This observation argues against Ga droplet formation because the droplets would be expected to form on fresh surfaces throughout the run. The diameter for catalyst-grown nanowires is determined by the size of the catalyst particle, which is not expected to vary as the growth proceeds. Diameters of MBE-grown wires depend on the nucleation conditions, which are widely variable on a local scale, and on the density of the nanowires on the substrate. As can be seen in comparing FESEM pictures in Figs. 2 and 5, widely spaced nanowires have nearly uniform diameter along their length, while closely spaced wires are significantly wider at the tips. This density effect is easily understood in terms of the model in Fig. 1. Ga atoms desorbing from a nanowire will continue into the vacuum for widely spaced nanowires, but are likely to strike a nearby wire when the wires are closely spaced. The recycling of these atoms will lead to higher incorporation on the sidewalls for a small but finite sidewall sticking coefficient. We have observed that lowering the RF power for the N_2 plasma source from 450 to 350 W at a constant N_2 flow of 2.1 μmol/s (3 sccm) also reduces the tendency for wires to increase in diameter as they grow. The lower RF power reduces atomic N flux out of the source, which in turn appears to lower the sidewall sticking coefficient.

The significant differences in the growth conditions typically used for catalytic and spontaneous growth also support the presence of different mechanisms. MBE-grown nanowires are grown at much higher temperatures than those used for planar epitaxial GaN MBE growth. For nanowire growth, somewhere between 10% and 60% of the impinging Ga flux is lost to re-evaporation. At these temperatures, sticking coefficients are below unity and therefore can vary significantly from plane to plane. There is not yet a direct measurement of the high-temperature sticking coefficients (or growth rate) for Ga on GaN for the two relevant crystallographic planes, the (0 0 0 1) *c*-plane and {1 1 0 0} *m*-planes. A recent MBE study of Ga wetting layers on GaN found that the Ga wetting layer was slower to accumulate and then to desorb on *m*-plane than on *c*-plane at 730 °C [29]. A combination experimental and theoretical study [30] of growth velocities on different planes also found higher growth velocity on *c*-planes than on *m*-planes for organometallic vapor phase epitaxial growth on three-dimensional patterned features. The high-temperature conditions for spontaneous nanowire growth are also expected to enhance surface diffusion of adatoms, which plays a significant role in our proposed growth mechanism. We have previously shown that inclusion of cations that alter surface diffusion also alters the nanowire morphology [4]. Finally, we note that catalyst growth is in general 100× to 1000× faster than spontaneous nanowire growth. The spontaneous growth is therefore expected to be driven more by equilibrium thermodynamics (e.g. minimizing surface energy) and less by kinetics (e.g. reactant supersaturation in a catalyst drop).

4. Conclusions

We have shown that spontaneous growth of GaN nanowires in MBE occurs by a process distinct from the more common catalyst-based, vapor–liquid–solid mechanism. MBE-grown nanowires propagate because of differences between the sticking coefficients of the Group III atoms on the nanowire tip and on the *m*-plane sidewalls. This model is supported qualitatively by the growth morphology and growth condition trends relative to layered GaN growth. The slow growth rate and re-evaporation of Ga are also to be expected in a process driven mostly by equilibrium thermodynamics. Alternative mechanisms involving the self-catalytic growth through Ga droplet formation are disproved by the absence of droplets, even after cooling in Ga flux, the reproducible and angular hexagonal cross-section of the nanowires, the slow growth rate, and the absence of nucleation throughout the run. The differential sticking coefficient model suggests that improvements in control of spontaneous nanowire growth are most likely to come from greater control of the nucleation process.

References

[1] J. Ristić, M.A. Sánchez-García, J.M. Ulloa, E. Calleja, J. Sánchez-Paramo, J.M. Calleja, U. Jahn, A. Trampert, K.H. Ploog, Phys. Stat. Sol. B 234 (2002) 717.
[2] F. Qian, Y. Li, S. Gradec¡;ak, D. Wang, C.J. Barrelet, C.M. Lieber, Nano Lett. 4 (2004) 1975.
[3] H.W. Li, A.H. Chin, M.K. Sunkara, Adv. Mater. 18 (2006) 216.
[4] K.A. Bertness, A. Roshko, N.A. Sanford, J.M. Barker, A.V. Davydov, J. Crystal Growth 287 (2006) 522.
[5] K.A. Bertness, A. Roshko, L.M. Mansfield, T.E. Harvey, N.A. Sanford, J. Crystal Growth 300 (2007) 94.
[6] K.A. Bertness, N.A. Sanford, J.M. Barker, J.B. Schlager, A. Roshko, A.V. Davydov, I. Levin, J. Electron. Mater 35 (2006) 576.
[7] J. Ristić, E. Calleja, S. Fernandez-Garrido, A. Trampert, U. Jahn, K.H. Ploog, M. Povoloskyi, A. Di Carlo, Phys. Stat. Sol. A 202 (2005) 367.
[8] K.L. Averett, J.E. Van Nostrand, J.D. Albrecht, Y.S. Chen, C.C. Yang, J. Vacuum Sci. Technol. B 25 (2007) 964.
[9] M. Yoshizawa, A. Kikuchi, M. Mori, N. Fujita, K. Kishino, Jpn. J. Appl. Phys. Part 2 36 (1997) L459.
[10] Y.H. Kim, J.Y. Lee, S.-H. Lee, J.-E. Oh, H.S. Lee, Appl. Phys. A Mater. Sci. Process 80 (2005) 1635.
[11] R. Meijers, T. Richter, R. Calarco, T. Stoica, H.P. Bochem, M. Marso, H. Luth, J. Crystal Growth 289 (2006) 381.
[12] S. Vaddiraju, A. Mohite, A. Chin, M. Meyyappan, G. Sumanasekera, B.W. Alphenaar, M.K. Sunkara, Nano Lett. 5 (2005) 1625.
[13] F. Qian, S. Gradec¡;ak, Y. Li, C.-Y. Wen, C.M. Lieber, Nano Lett. 5 (2005) 2287.
[14] C.Y. Nam, D. Tham, J.E. Fischer, Appl. Phys. Lett. 85 (2004) 5676.
[15] P.V. Radovanovic, K.G. Stamplecoskie, B.G. Pautler, J. Am. Chem. Soc. 129 (2007) 10980.
[16] H.-J. Choi, J.C. Johnson, R. He, S. Lee, F. Kim, P. Pauzauskie, J. Goldberger, R.J. Saykally, P. Yang, J. Phys. Chem. B 2003 (2003) 8721.
[17] M.Q. He, I. Minus, P.Z. Zhou, S.N. Mohammed, J.B. Halpern, R. Jacobs, W.L. Sarney, L. Salamanca-Riba, R.D. Vispute, Appl. Phys. Lett. 77 (2000) 3731.
[18] Y. Inoue, T. Hoshino, S. Takeda, K. Ishino, A. Ishida, H. Fujiyasu, H. Kominami, H. Mimura, Y. Nakanishi, S. Sakakibara, Appl. Phys. Lett. 85 (2004) 2340.
[19] S.D. Hersee, X.Y. Sun, X. Wang, Nano Lett. 6 (2006) 1808.
[20] P. Deb, H. Kim, V. Rawat, M. Oliver, S. Kim, M. Marshall, E. Stach, T. Sands, Nano Lett. 5 (2005) 1847.
[21] M. Boćkowski, I. Grzegory, G. Kamler, B. Łucznik, S. Krukowski, M. Wróblewski, P. Kwiatkowski, K. Jasik, S. Porowski, J. Crystal Growth 305 (2007) 414.
[22] N. Thillosen, K. Sebald, H. Hardtdegen, R. Meijers, R. Calarco, S. Montanari, N. Kaluza, J. Gutowski, H. Lüth, Nano Lett. 6 (2006) 704.
[23] L. Cerutti, J. Ristić, S. Fernandez-Garrido, E. Calleja, A. Trampert, K.H. Ploog, S. Lazic, J.M. Calleja, Appl. Phys. Lett. 88 (2006).
[24] J. Ristić, E. Calleja, M.A. Sánchez-García, J.M. Ulloa, J. Sánchez-Paramo, J.M. Calleja, U. Jahn, A. Trampert, K.H. Ploog, Phys. Rev. B 68 (2003) 125305-1.
[25] H. Sekiguchi, T. Nakazato, A. Kikuchi, K. Kishino, J. Crystal Growth 300 (2007) 259.
[26] E. Calleja, M.A. Sánchez-García, F.J. Sánchez, F. Calle, F.B. Naranjo, E. Muñoz, U. Jahn, K. Ploog, Phys. Rev. B 62 (2000) 16826.
[27] A. Kikuchi, M. Kawai, M. Tada, K. Kishino, Jpn. J. Appl. Phys. Part 2 43 (2004) L1524.
[28] F. Schulze, O. Kisel, A. Dadgar, A. Krtschil, J. Blasing, M. Kunze, I. Daumiller, T. Hempel, A. Diez, R. Clos, J. Christen, A. Krost, J. Crystal Growth 299 (2007) 399.
[29] S. Choi, T.H. Kim, H.O. Everitt, A. Brown, M. Losurdo, G. Brun, A. Moto, J. Vacuum Sci. Technol. B 25 (2007) 969.
[30] D. Du, D.J. Srolovitz, M.E. Coltrin, C.C. Mitchell, Phys. Rev. Lett. 95 (2005) 155503.